Local splines of the Second and Third Order, Complex-valued Splines and Image Processing

I.G. Burova, E.F. Muzafarova, I.I.Narbutovskikh

Abstract— This paper is devoted to the local complex-valued spline interpolation in a circle and image processing using local polynomial and non-polynomial splines. We consider local complex-valued spline interpolation, constructed by using tensor product. For constructing the tensor product we use local basis splines of two variables: a radial variable and an angular variable. The approximation is constructed separately in each elementary segment, formed by two arcs and two line segments. For the approximation of a complex-valued function we use the values of the function in several nodes near this elementary segment and the basis splines. The order of the approximation depends on the properties of splines of one variable which we use in the tensor product. In this paper we suggest using local exponential, local trigonometrical and local polynomial splines of the second and third order of approximation. The local spline interpolation is the most convenient for the approximation and visualization of functions and they may be applied to solving various problems. In this paper we focus on the problem of enlarging images using the local splines.

Keywords—complex-valued splines, polynomial spline, exponential spline, trigonometric spline, tensor product, approximation, interpolation, image processing

I. Introduction

LOCAL polynomial splines (see [1-3]) are widely used for solving different problems. In [2], to approximate the functions of two variables, using the tensor product is suggested. Sometimes it is necessary to use complex splines. Ahlberg, Nilson and Walsh (see [4, 5]) constructed analytic splines.

Many researchers made a significant contribution to the development of approximation theory of complex-valued functions [6-23]. A great contribution to the development of the theory of spline approximation was made by Walsh [1, 3, 4, 6]. L. Reichel [7] considered the selection of polynomial bases for the polynomial approximation of analytic functions on bounded, simply connected regions in the complex plane. Complex cubic splines that interpolate a function given at the nodal points have been studied in detail in [4].

I.G.Burova is with the St. Petersburg State University,7/9 Universitetskaya nab., 199034, St. Petersburg, Russia (corresponding author, e-mail: i.g.burova@spbu.ru).

E.F.Muzafarova is with the St. Petersburg State University, 7/9 Universitetskaya nab., 199034, St. Petersburg, Russia (e-mail: e.muzafar@yandex.ru)

I.I.Narbutovskikh is with the St. Petersburg State University, 7/9 Universitetskaya nab., 199034, St. Petersburg, Russia (e-mail: i.narbutovskikh@gmail.com)

Accurate modeling of an RF power amplifier and/or its inverse is the core element of every digital predistortion system. In [20] the authors suggest an interesting alternative to the family of classic polynomial models, in particular they suggest piecewise models, which divide the magnitude range into segments and define gain/phase-distortion through complex-valued functions on a per-segment basis.

A complex-valued cubic spline is used in [23] to directly interpolate the complex exponentials of the phase angles at the nodal points. Shape sensitivity measures the impact of small perturbations of geometric features of a problem on certain quantities of interest. The shape sensitivity of PDE (partial differential equation) constrained output functionals is derived with the help of shape gradients. In electromagnetic scattering problems, the standard procedure of the Lagrangian approach cannot be applied because of the solution of the state problem is complex valued.

It should be noted that for the solution of various problems the authors often use B-splines (see [8-10, 13, 15, 21, 24]). In [13] the authors derive a closed-form formula of the shape gradient of a generic output functional constrained by Maxwell's equations. They employ cubic B-splines to model local deformations of the geometry.

In this paper we use complex splines to approximate a function defined in the complex plane. Instead of the Lagrange interpolation polynomials and analytic splines, we use the local spline interpolation. For the construction of the approximation of complex-valued function we use the tensor product of splines of one variable. The construction of approximations of the functions of two variables can be constructed similarly using the tensor product of splines of one variable.

This paper is a continuation of the research initiated by the author in [25]. In the second section we construct local polynomial interpolation splines on a line. These splines are continuous ones. The error of approximation with these splines is the second and third order. In the third section, we consider the construction and properties of continuous local exponential interpolation splines on the circle. We construct an approximation of real and imaginary parts of a complex-valued function in polar coordinates using a tensor product. We can use all these local splines for compressing and restoring images. Another task is to resize the image in accordance with the properties of various modern displays. In the fourth section, we discuss the application of our splines to enlarge images.

II. Approximation on a Line

Let m, r, r_1 be natural numbers, such that $r + r_1 = m + 1$. Let $\{x_j\}$ be a sequence of distinct points, $a = x_0 < \cdots < x_{j-1} < x_j < x_{j+1} < ..x_n = b$. Suppose f is a function such that $f \in C^{m+1}[a, b]$, and f is given in nodes x_j, $j = 0, \dots, m$. Suppose φ_i, $i = 0, \dots, m$. We propose that the system of functions φ_i forms a Chebyshev system on $[x_j, x_{j+1}]$. We construct approximation $\tilde{f}(x)$ of the function $f(x)$ with local splines separately on every $[x_j, x_{j+1}]$ in the following form:

$$\tilde{f}(x) = \sum_s f(x_s)\,\omega_s(x), \qquad x \in [x_j, x_{j+1}],$$

where $\omega_s(x)$ we obtain as a solution of the system of equations

$$\tilde{f}(x) = f(x),\ f(x) = \varphi_0(x), \varphi_1(x), \dots, \varphi_m(x). \qquad (1)$$

When approximating a function on a finite interval $[a, b]$, it is necessary to distinguish the use of the left and right splines. They have the same approximation order, but some of them use the function values: only to the right of the left end of the interval; or only to the left of the right end of the interval. Combining the application of these splines we have the ability to use the values of the function only in the grid nodes on the interval. In the polynomial case when $m = 1$ on the uniform grid of nodes, the approximation error is known. (see [2]). If $m = 1$ $(\varphi_0(x) = 1, \varphi_1(x) = x)$ the approximation error is the following:

$$|\tilde{f}(x) - f(x)| \le \frac{1}{8!} h^2 \|f''\|_{[x_j, x_{j+1}]}, \quad x \in [x_j, x_{j+1}].$$

Suppose $m = 2$. In the following examples, we consider basic splines generated by different systems of functions $\{\varphi_i\}$.

A. About the Left Splines

We choose a support of the basic splines ω_j so that, $supp\ \omega_j = [x_{j-1}, x_{j+2}]$. Knowing $f(x_{j-1})$, $f(x_j)$, $f(x_{j+1})$ we construct an approximation of the function $f(x)$, $x \in [x_j, x_{j+1}]$, with the left-side basic splines in the form:

$$\tilde{f}(x) = f(x_{j-1})\,\omega_{j-1}(x) + f(x_j)\,\omega_j(x) + f(x_{j+1})\,\omega_{j+1}(x). \qquad (2)$$

Example 1.1. Basic splines $\omega_{j-1}(x)$, $\omega_j(x)$, $\omega_{j+1}(x)$, obtained from system (1) where $\varphi_i = x^i$, $i = 0,1.2,$ $x \in [x_j, x_{j+1}]$, will be the following:

$$\omega_{j-1}(x) = \frac{(x - x_j)(x - x_{j+1})}{(x_{j-1} - x_j)(x_{j-1} - x_{j+1})},$$

$$\omega_j(x) = \frac{(x - x_{j-1})(x - x_{j+1})}{(x_j - x_{j-1})(x_j - x_{j+1})},$$

$$\omega_{j+1}(x) = \frac{(x - x_{j-1})(x - x_j)}{(x_{j+1} - x_{j-1})(x_{j+1} - x_j)}.$$

Plots of basic functions $\omega_j(x)$, $\omega_{j+1}(x)$, $\omega_{j-1}(x)$ are given in Fig.1.

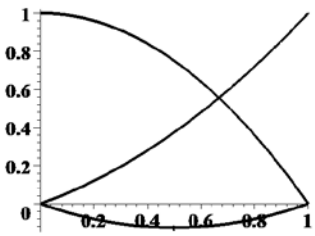

Fig. 1. Plots of basic functions $\omega_j(x), \omega_{j+1}(x), \omega_{j-1}(x)$.

The basis spline $\omega_j(x)$ can be written in the form:

$$\omega_j(x) = \begin{cases} \dfrac{(x - x_{j+1})(x - x_{j+2})}{(x_j - x_{j+1})(x_j - x_{j+2})}, & x \in [x_{j+1}, x_{j+2}], \\ \dfrac{(x - x_{j-1})(x - x_{j+1})}{(x_j - x_{j-1})(x_j - x_{j+1})}, & x \in [x_j, x_{j+1}], \\ \dfrac{(x - x_{j-2})(x - x_{j-1})}{(x_j - x_{j-2})(x_j - x_{j-1})}, & x \in [x_{j-1}, x_j], \end{cases}$$

and $\omega_j(x) = 0$, $x \notin [x_{j-1}, x_{j+2}]$.

A plot of the basic spline $\omega_j(x)$ is shown in Fig. 2. Approximation (2) can be applied to $[x_j, x_{j+1}]$, $j = 1, 2, \dots, n-1$. Formula (2) provides continuous approximation $\tilde{f}(x)$ of the function $f(x)$ on the interval $[a + h, b]$.

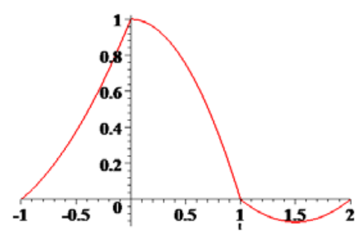

Fig.2. Plot of $\omega_j(x)$, $supp\ \ \omega_j = [x_{j-1}, x_{j+2}]$.

Let $h = (b - a)/n$. The error of the approximation function $f(x)$ with spline $\tilde{f}(x)$ obtained with (2) will be the following:

$$|\tilde{f}(x) - f(x)| \le \frac{0.385}{3!} h^3 \|f'''\|_{[x_{j-1}, x_{j+1}]}, \quad x \in [x_j, x_{j+1}].$$

If $x=x_j+\tau h$, $x_{j+1}=x_j+h$, $x_{j-1}=x_j-h$ on the uniform grid of nodes with step h formulae $w_{j-1}(x), w_j(x), w_{j+1}(x)$ can be written in the form:

$$w_{j-1}(x_j+\tau h)=\frac{(\tau-1)\tau}{2},\ w_{j+1}(x_j+\tau h)=\frac{(\tau+1)\tau}{2},$$

$w_j(x_j+\tau h)=-(\tau+1)(\tau-1)$, where $0\le\tau\le 1$.

Example 1.2. Basic splines $\omega^T_{j-1}(x), \omega^T_j(x), \omega^T_{j+1}(x)$, obtained from system (1) where $\varphi_0=1$, $\varphi_1=\sin(x)$, $\varphi_2=\cos(x)$, $x\in[x_j,x_{j+1}]$, will be the following:

$$\omega^T_j(x)=\frac{\sin(x-x_{j+1})-\sin(x_{j-1}-x_{j+1})-\sin(x-x_{j-1})}{\sin(x_j-x_{j+1})-\sin(x_{j-1}-x_{j+1})-\sin(x_j-x_{j-1})},$$

$$\omega^T_{j+1}(x)=\frac{\sin(x-x_{j-1})-\sin(x-x_j)-\sin(x_j-x_{j-1})}{\sin(x_j-x_{j+1})-\sin(x_j-x_{j-1})-\sin(x_{j-1}-x_{j+1})},$$

$$\omega^T_{j-1}(x)=\frac{\sin(x-x_j)+\sin(x_j-x_{j+1})-\sin(x-x_{j+1})}{\sin(x_j-x_{j+1})-\sin(x_j-x_{j-1})-\sin(x_{j-1}-x_{j+1})}.$$

The error of the approximation function $f(x)$ with spline $\tilde f(x)$ obtained with (2) will be the following:
$|\tilde f(x)-f(x)|\le K_1 h^3\|f'''+f'\|_{[x_{j-1},x_{j+1}]}$, $x\in[x_j,x_{j+1}]$.

where $K_1>0$. The way of obtainin the order of approximation for nonpolynomial splines is given in paper [26]. Plots of basic functions $\omega^T_{j-1}(x), \omega^T_j(x), \omega^T_{j+1}(x)$ are given in Fig. 3.

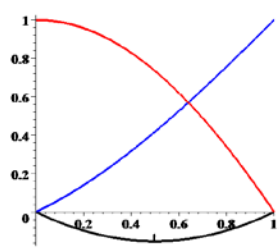

Fig. 3. Plots of basic function $\omega^T_{j-1}(x), \omega^T_j(x), \omega^T_{j+1}(x)$.

Example 1.3. Basic exponential splines $\omega^E_{j-1}(x)$, $\omega^E_j(x)$, $\omega^E_{j+1}(x)$ obtained from system (1) where $\varphi_0=1$, $\varphi_1=e^x, \varphi_2=e^{2x}$, $x\in[x_j,x_{j+1}]$, will be the following:

$$\omega^E_j(x)=\frac{(e^x-e^{x_{j-1}})(e^x-e^{x_{j+1}})}{(e^{x_j}-e^{x_{j-1}})(e^{x_j}-e^{x_{j+1}})},$$

$$\omega^E_{j+1}(x)=\frac{(e^x-e^{x_j})(e^x-e^{x_{j-1}})}{(e^{x_j}-e^{x_{j+1}})(e^{x_{j-1}}-e^{x_{j+1}})},$$

$$\omega^E_{j-1}(x)=\frac{(e^x-e^{x_j})(e^x-e^{x_{j+1}})}{(e^{x_{j-1}}+e^{x_{j+1}})(e^{x_j}-e^{x_{j-1}})}.$$

The error of the approximation function $f(x)$ with spline $\tilde f(x)$ obtained with (2) will be the following:
$|\tilde f(x)-f(x)|\le K_2 h^3\|f'''-3f''+2f'\|_{[x_{j-1},x_{j+1}]}$, $x\in[x_j,x_{j+1}]$.

where $K_2>0$. Plots of basic functions $\omega^E_{j-1}(x)$, $\omega^E_j(x)$, $\omega^E_{j+1}(x)$ are given in Fig. 4.

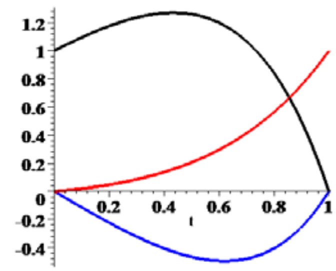

Fig. 4. Plots of basic functions $\omega^E_{j-1}(x)$, $\omega^E_j(x)$, $\omega^E_{j+1}(x)$.

Example 1.4 .Basis splines $\omega^e_{j-1}(x)$, $\omega^e_j(x)$, $\omega^e_{j+1}(x)$, obtained from system (1) where $\varphi_0=1$, $\varphi_1=e^{-x}$, $\varphi_2=e^x$, $x\in[x_j,x_{j+1}]$, will be the following:

$$\omega^e_j(x)=\frac{e^{x_j}(e^x-e^{x_{j-1}})(e^x-e^{x_{j+1}})}{e^x(e^{x_j}-e^{x_{j+1}})(e^{x_j}-e^{x_{j-1}})},$$

$$\omega^e_{j+1}(x)=\frac{e^{x_{j+1}}(e^x-e^{x_j})(e^x-e^{x_{j-1}})}{e^x(e^{x_{j-1}}-e^{x_{j+1}})(e^{x_j}-e^{x_{j+1}})},$$

$$\omega^e_{j-1}(x)=\frac{-e^{x_{j-1}}(e^x-e^{x_j})(e^x-e^{x_{j+1}})}{e^x(e^{x_{j-1}}-e^{x_{j+1}})(e^{x_j}-e^{x_{j-1}})}.$$

The error of the approximation function $f(x)$ with spline $\tilde f(x)$ obtained with (2) will be the following:
$|\tilde f(x)-f(x)|\le K_3 h^3\|f'''-f'\|_{[x_{j-1},x_{j+1}]}$, $x\in[x_j,x_{j+1}]$.

where $K_3>0$. Plots of basic functions $\omega^e_{j-1}(x)$, $\omega^e_j(x)$, $\omega^e_{j+1}(x)$ are given in Fig. 5.

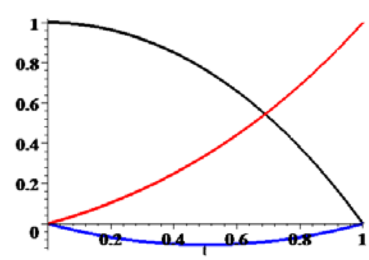

Fig. 5. Plots of basic functions $\omega^e_{j-1}(x)$, $\omega^e_j(x)$, $\omega^e_{j+1}(x)$.

B. *About the Right Splines*

Suppose $supp\ \omega_j=[x_{j-2},x_{j+1}]$. Knowing $f(x_j)$, $f(x_{j+1})$, $f(x_{j+2})$ we construct an approximation of the function $f(x), x\in[x_j,x_{j+1}]$ in the form:

$$\tilde{f}(x) = f(x_j)\,\omega_j(x) + f(x_{j+1})\,\omega_{j+1}(x) + f(x_{j+2})\,\omega_{j+2}(x). \quad (3)$$

Example 2.1. Basic splines $\omega_j(x)$, $\omega_{j+1}(x)$, $\omega_{j+2}(x)$, obtained from system (1) where $\varphi_i = x^i$, $i = 0,1.2$, $[x_j, x_{j+1}]$, will be the following:

$$\omega_j(x) = \frac{(x - x_{j+2})(x - x_{j+1})}{(x_j - x_{j+2})(x_j - x_{j+1})},$$

$$\omega_{j+1}(x) = \frac{(x - x_{j+2})(x - x_j)}{(x_{j+1} - x_{j+2})(x_{j+1} - x_j)},$$

$$\omega_{j+2}(x) = \frac{(x - x_{j+1})(x - x_j)}{(x_{j+2} - x_{j-1})(x_{j+2} - x_j)}.$$

$$|\tilde{f}(x) - f(x)| \le \frac{0.385}{3!} h^3 \|f'''\|_{[x_j,\, x_{j+2}]}, \quad x \in [x_j, x_{j+1}].$$

This approximation can be applied to $[x_j, x_{j+1}]$, $j = 0, 1, \dots, n-2$, and it provides continuous approximation $\tilde{f}(x)$ of function $f(x)$ on the interval following form:

$$\omega_j(x) = \begin{cases} \dfrac{(x - x_{j+1})(x - x_{j+2})}{(x_j - x_{j+1})(x_j - x_{j+2})}, & x \in [x_j, x_{j+1}], \\ \dfrac{(x - x_{j-1})(x - x_{j+1})}{(x_j - x_{j-1})(x_j - x_{j+1})}, & x \in [x_{j-1}, x_j], \\ \dfrac{(x - x_{j-2})(x - x_{j-1})}{(x_j - x_{j-2})(x_j - x_{j-1})}, & x \in [x_{j-2}, x_{j-1}], \end{cases}$$

and $\omega_j(x) = 0$, $x \notin [x_{j-2}, x_{j+1}]$.

A plot of the basic spline $\omega_j(x)$ is shown in Fig. 6.

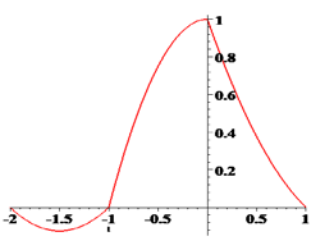

Fig.6. Plot of $\omega_j(x)$, *supp* $\omega_j = [x_{j-2}, x_{j+1}]$.

Example 2.2. Basic splines $\omega_j^T(x)$, $\omega_{j+1}^T(x)$, $\omega_{j+2}^T(x)$, obtained from system (1) where $\varphi_0 = 1$, $\varphi_1 = \sin(x)$, $\varphi_2 = \cos(x)$, $x \in [x_j, x_{j+1}]$, will be the following:

$$\omega_j^T(x) = \frac{\sin(x_{j+1} - x_{j+2}) - \sin(x - x_{j+2}) + \sin(x - x_{j+1})}{\sin(x_j - x_{j+1}) - \sin(x_j - x_{j+2}) + \sin(x_{j+1} - x_{j+2})},$$

$$\omega_{j+1}^T(x) = \frac{\sin(x - x_{j+2}) - \sin(x - x_j) - \sin(x_j - x_{j+2})}{\sin(x_j - x_{j+1}) - \sin(x_j - x_{j+2}) + \sin(x_{j+2} - x_{j+1})},$$

$$\omega_{j+2}^T(x) = -\frac{\sin(x - x_{j+1}) - \sin(x_j - x_{j+1}) - \sin(x - x_j)}{\sin(x_j - x_{j+1}) - \sin(x_j - x_{j+2}) + \sin(x_{j+1} - x_{j+2})}.$$

The error of the approximation function $f(x)$ with spline $\tilde{f}(x)$ obtained with formula (3) will be the following:

$$|\tilde{f}(x) - f(x)| \le C_1 h^3 \|f''' + f'\|_{[x_j,\, x_{j+2}]}, \quad x \in [x_j, x_{j+1}].$$

where $C_1 > 0$.

Example 2.3. Basic splines $\omega_j^E(x), \omega_{j+1}^E(x), \omega_{j+2}^E(x)$, obtained from system (1) where $\varphi_0 = 1$, $\varphi_1 = e^x$, $\varphi_2 = e^{2x}$, $x \in [x_j, x_{j+1}]$, will be the following:

$$\omega_j^E(x) = \frac{(e^x - e^{x_{j+1}})(e^x - e^{x_{j+2}})}{(e^{x_j} - e^{x_{j+1}})(e^{x_j} - e^{x_{j+2}})},$$

$$\omega_{j+1}^E(x) = \frac{(e^x - e^{x_{j+2}})(e^x - e^{x_j})}{(e^{x_{j+2}} - e^{x_{j+1}})(e^{x_j} - e^{x_{j+1}})},$$

$$\omega_{j+2}^E(x) = -\frac{(e^x - e^{x_{j+1}})(e^x - e^{x_j})}{(e^{x_{j+2}} - e^{x_{j+1}})(e^{x_j} - e^{x_{j+2}})}.$$

The error of the approximation function $f(x)$ with spline $\tilde{f}(x)$ obtained with formula (3) will be the following:

$$|\tilde{f}(x) - f(x)| \le C_2 h^3 \|f''' - 3f'' + 2f'\|_{[x_j,\, x_{j+2}]}, \quad x \in [x_j, x_{j+1}].$$

where $C_2 > 0$.

Example 2.4. Basic splines $\omega_j^e(x)$, $\omega_{j+1}^e(x)$, $\omega_{j+2}^e(x)$, obtained from system (1) where $\varphi_0 = 1$, $\varphi_1 = e^{-x}, \varphi_2 = e^x$, $x \in [x_j, x_{j+1}]$, will be the following:

$$\omega_j^e(x) = \frac{e^{x_j}(e^x - e^{x_{j+1}})(e^x - e^{x_{j+2}})}{e^x(e^{x_j} - e^{x_{j+1}})(e^{x_j} - e^{x_{j+2}})},$$

$$\omega_{j+1}^e(x) = \frac{e^{x_{j+1}}(e^x - e^{x_{j+2}})(e^x - e^{x_j})}{e^x(e^{x_{j+2}} - e^{x_{j+1}})(e^{x_j} - e^{x_{j+1}})},$$

$$\omega_{j+2}^e(x) = -\frac{e^{x_{j+2}}(e^x - e^{x_{j+1}})(e^x - e^{x_j})}{e^x(e^{x_{j+2}} - e^{x_{j+1}})(e^{x_j} - e^{x_{j+2}})}.$$

The error of the approximation function $f(x)$ with spline $\tilde{f}(x)$ obtained with (3) will be the following:

$$|\tilde{f}(x) - f(x)| \le C_3 h^3 \|f''' - f'\|_{[x_j,\, x_{j+2}]}, \quad x \in [x_j, x_{j+1}].$$

where $C_3 > 0$.

The following Lemma shows the relations between non-polynomial and polynomial basis splines. It is not difficult to formulate a similar lemma for right splines.

Lemma. Let $t \in [0,1]$, $x_{j+1} = x_j + h$, $x = x_j + t\,h$. The following relationships are valid:

1) For trigonometrical basic splines

$$\omega_j^T(t) = -(t-1)(t+1) + O(h^2),$$

$$\omega_{j+1}^T(t) = \frac{t(t+1)}{2} + O(h^2),$$

$$\omega_{j-1}^{T}(t) = \frac{t(t-1)}{2} + O(h^2),$$

2) *For exponential basic splines (example 1.3)*

$$\omega_{j}^{E}(t) = -(t-1)(t+1) + O(h),$$

$$\omega_{j+1}^{E}(t) = \frac{t(t+1)}{2} + O(h),$$

$$\omega_{j-1}^{E}(t) = \frac{t(t-1)}{2} + O(h),$$

3) *For exponential basic splines (example 1.4)*

$$\omega_{j}^{e}(t) = -(t-1)(t+1) + O(h),$$

$$\omega_{j+1}^{e}(t) = \frac{t(t+1)}{2} + O(h),$$

$$\omega_{j-1}^{e}(t) = \frac{t(t-1)}{2} + O(h).$$

Proof. Using the Taylor expansion in the vicinity of $h = 0$, we obtain the required relations.

Remark. Similar relations are valid for the basic splines from examples 2.1-2.4.

These approximations are easy to apply both on a uniform and non-uniform grid (see [27]). Let us compare the approximations constructed on a uniform grid with step h and on a non-uniform grid constructed using the formula:

$$\int_{x_j}^{x_{j+1}} \sqrt{1+(f'(x))^2}\, dx = I_0.$$

The next node x_{j+1} we find after solving this non-linear equation.

Figs. 7-10 shows the errors of approximation of function $f(x) = 1/(1+25x^2)$. The approximations were constructed with splines from examples 1.1-1.4, 2-1-2.4. Figs. 8, 10 shows the errors of approximation on the uniform grids when $n = 10, 20$, $[a,b] = [-1,1]$. Figs. 7, 9 shows the errors of approximation on the non-uniform grids when $n = 10,20$, $[a,b] = [-1,1]$.

The results show that approximations with basic exponential splines $\omega_{j-1}^{E}(x)$, $\omega_{j}^{E}(x)$, $\omega_{j+1}^{E}(x)$ gives greater error in comparison to other splines when n is not very big. Fig.10 shows the errors of approximation of function $f(x) = \sin(5x)$ on the uniform grid when $n = 20$, $[a,b] = [-1,1]$. The approximations were constructed with splines from examples 1.1-1.4, 2-1-2.4.

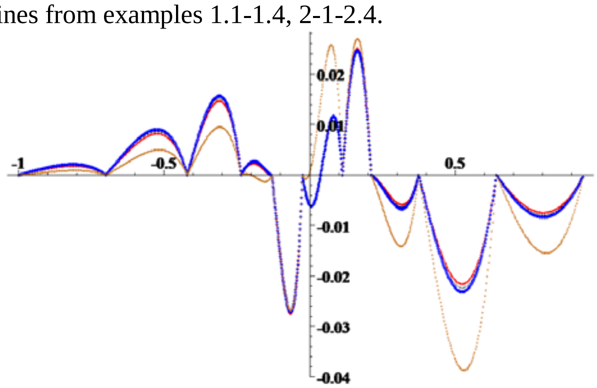

Fig.7. The errors of approximation of the function $1/(1+25x^2)$ on the non-uniform grid ($n = 10$).

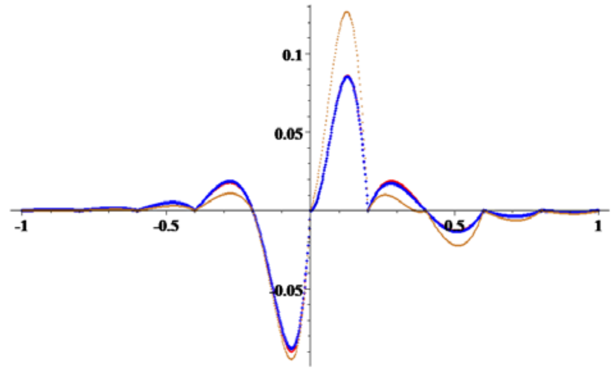

Fig.8. The errors of approximation of the function $1/(1+25x^2)$ on the uniform grid ($n = 10, h = 0.2$).

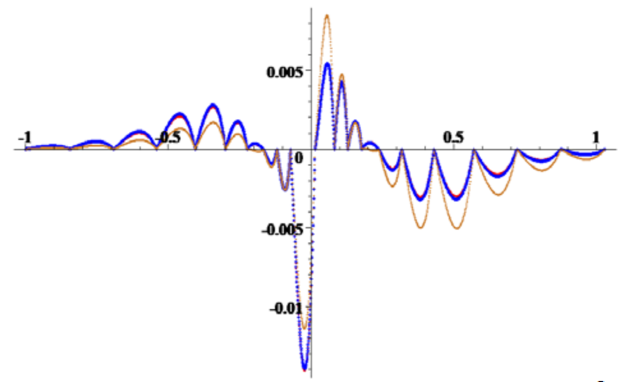

Fig.9. The errors of approximation of the function $1/(1+25x^2)$ on the non-uniform grid ($n = 20$).

Table 1 shows the maximum in absolute values of the errors of approximation of function $1/(1+25x^2)$ with different splines (polynomial, trigonometrical, exponential (from examples 1.3, 2.3), exponential (from examples 1.4, 2,4) on the uniform grid (10 and 20 points of the interpolation on [-1,1]). Table 2 shows the maximum in absolute values of the errors of approximation of function $1/(1+25x^2)$ with different splines (polynomial, trigonometrical, exponential (from examples 1.3, 2.3), exponential (from example 1.4, 2.4) on the non-uniform grid constructed with our formula (10 and 20 points of the interpolation on [-1,1]).

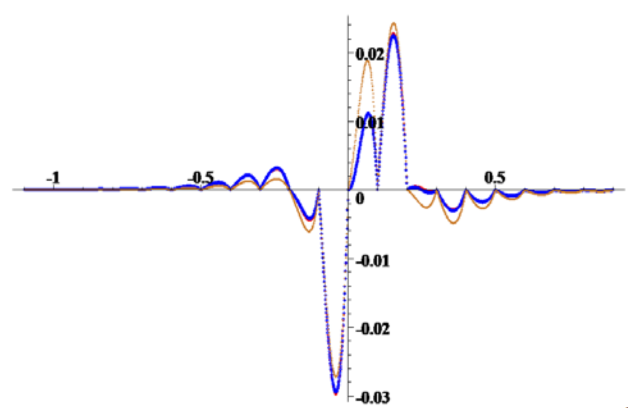

Fig.10. The errors of approximation of the function $1/(1+25x^2)$ on the uniform grid ($n = 20$).

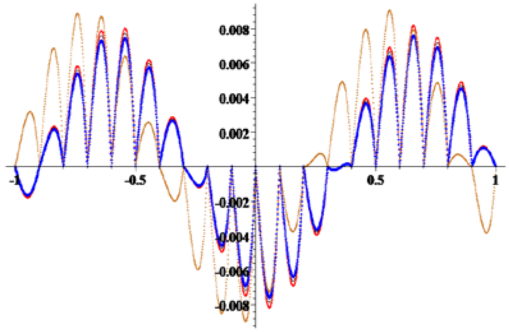

Fig.11. The errors of approximation of the function $\sin(5x)$ on the uniform grid ($n = 20$).

TABLE 1. ERRORS OF APPROXIMATION ON THE UNIFORM GRID

n	Polinomial	Trigonometric	Exp (example 1.3)	Exp (example 1.4)
10	$0.90 \cdot 10^{-1}$	$0.90 \cdot 10^{-1}$	$0.12 \cdot 10^{0}$	$0.90 \cdot 10^{-1}$
20	$0.30 \cdot 10^{-1}$	$0.29 \cdot 10^{-1}$	$0.27 \cdot 10^{-1}$	$0.30 \cdot 10^{-1}$

TABLE 2. ERRORS OF APPROXIMATION ON THE NON-UNIFORM GRID

n	Polinomial	Trigonometric	Exp (example 1.3)	Exp (example 1.4)
10	$0.27 \cdot 10^{-1}$	$0.27 \cdot 10^{-1}$	$0.39 \cdot 10^{-1}$	$0.27 \cdot 10^{-1}$
20	$0.14 \cdot 10^{-1}$	$0.14 \cdot 10^{-1}$	$0.11 \cdot 10^{-1}$	$0.14 \cdot 10^{-1}$

The comparison of the results presented in Tables 1 and 2 show that the use of a non-uniform grid reduces the approximation error if the number of grid nodes does not change.

III. APPROXIMATION OF A COMPLEX-VALUED FUNCTION

Suppose a complex-valued analytical function is given at nodes on unit disc K. Let m, n be integers. For the construction of grid G we consider n circles in the disc of radius 1 with a center of 0, and get m points $P_{j,k}$ on the boundary on disc K. We connect these points by lines with a center of 0 of disc K. We plot lines from the centre to the edge. The points at which those lines cross each circle form the grid nodes G. We plot a radial grid in disc K with step $h = \frac{1}{m}$ on the radial variable and $h_1 = \frac{2\pi}{n}$ on the angular variable. Now we get a grid of nodes (r_j, φ_k) such that $r_j = jh$, $\varphi_k = kh_1$, where $j = 0, \ldots, m$, $k = 0, \ldots, n$. Then unit disc K is represented as a union of the elementary curvilinear quadrangles. Suppose the numeration of the angular variable is in a counterclockwise order, the numeration of the radial variable is selected from the center to the edge.

Denote the elementary curvilinear quadrangle by $S_{j,k}$ (see Fig. 12), formed by two arcs with boundary points $P_{j,k}$, $P_{j,k+1}$ and $P_{j+1,k}$, $P_{j+1,k+1}$, and two line segments with boundary points $P_{j,k}, P_{j+1,k}$ and $P_{j,k+1}, P_{j+1,k+1}$. Thus, the vertices of this curvilinear quadrangle will be denoted as follows: $P_{j,k} = (r_j, \varphi_k)$, $P_{j,k+1} = (r_j, \varphi_{k+1})$, $P_{j+1,k} = (r_{j+1}, \varphi_k)$, $P_{j+1,k+1} = (r_{j+1}, \varphi_{k+1})$. Suppose values of a complex function are given at grid nodes. In constructing the approximation, we will use real splines along the radial component. Here we can apply any splines presented in the previous section.

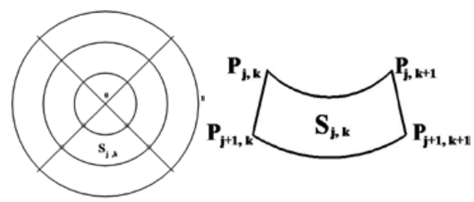

Fig.12. Grid in the disc (left); elementary curvilinear quadrangle (right).

The approximation $\tilde{u}_1(\rho,\varphi)$ of function $u(\rho,\varphi)$ is constructed separately in each elementary segment $S_{j,k}$ as follows:

$$
\begin{aligned}
\tilde{u}_1(\rho,\varphi) &= u(r_j,\varphi_k)w_j(\rho)v_k(\varphi) + \\
&+ u(r_{j+1},\varphi_k)w_{j+1}(\rho)v_k(\varphi) + \\
&+ u(r_j,\varphi_{k+1})w_j(\rho)v_{k+1}(\varphi) + \\
&+ u(r_{j+1},\varphi_{k+1})w_{j+1}(\rho)v_{k+1}(\varphi), \quad (\rho,\varphi) \in S_{j,k},
\end{aligned}
\tag{4}
$$

where

$$
w_j(\rho) = \frac{r_{j+1} - \rho}{r_{j+1} - r_j}, \; w_{j+1}(\rho) = \frac{\rho - r_j}{r_{j+1} - r_j}, \tag{5}
$$

and

$$
v_k(\varphi) = \frac{e^{\varphi_{k+1} I} - e^{\varphi I}}{e^{\varphi_{k+1} I} - e^{\varphi_k I}},
$$

$$
v_{k+1}(\varphi) = \frac{e^{\varphi I} - e^{\varphi_k I}}{e^{\varphi_{k+1} I} - e^{\varphi_k I}}.
$$

The basic function $v_k(\varphi)$ may be written in the following form: $v_k(\varphi) = A_k(\varphi) + I \cdot B_k(\varphi)$, where

$$
\begin{aligned}
A_k(\varphi) &= (-\cos(-2\varphi_{k+1} + \varphi) + \\
&+ 2\cos(-\varphi_{k+1} + \varphi - \varphi_k) + \cos(2\varphi_k - \varphi_{k+1}) - \\
&- \cos(-2\varphi_k + \varphi) + \cos(\varphi_{k+1}) - \\
&- 2\cos(\varphi_k))/(2 - 2\cos(\varphi_k - \varphi_{k+1})), \\
B_k(\varphi) &= (-\sin(2\varphi_k - \varphi_{k+1}) - \\
&- \sin(-2\varphi_{k+1} + \varphi) + 2\sin(-\varphi_{k+1} + \varphi - \varphi_k) - \\
&\sin(-2\varphi_k + \varphi) - \sin(\varphi_{k+1}) + \\
&+ 2\sin(\varphi_k))/(2 - 2\cos(\varphi_k - \varphi_{k+1})).
\end{aligned}
$$

The basic function $v_{k+1}(\varphi)$ may be written in the following form: $v_{k+1}(\varphi) = A_{k+1}(\varphi) + I \cdot B_{k+1}(\varphi)$, where

$$A_{k+1}(\varphi) = (-\cos(\varphi_k + 2\varphi_{k+1}) + 2\cos(2\varphi_k + \varphi_{k+1}) + \cos(2\varphi_{k+1} + \varphi) - 2\cos(\varphi_{k+1} + \varphi + \varphi_k) - \cos(3\varphi_k) + \cos(2\varphi_k + \varphi))/(2 - 2\cos(\varphi_k - \varphi_{k+1})),$$

$$B_{k+1}(\varphi) = ((\sin(\varphi_k + 2\varphi_{k+1}) - 2\sin(2\varphi_k + \varphi_{k+1}) - \sin(2\varphi_{k+1} + \varphi) + 2\sin(\varphi_{k+1} + \varphi + \varphi_k) + \sin(3\varphi_k) - \sin(2\varphi_k + \varphi))/(2 - 2\cos(\varphi_k - \varphi_{k+1})).$$

Plots of real and imaginary parts of the basic function $V_{j,k}(\rho,\varphi) = \omega_j(\rho)\, v_k(\varphi)$ are given in Fig. 13 and Fig. 14. The relief of basic function is given in Fig. 15.

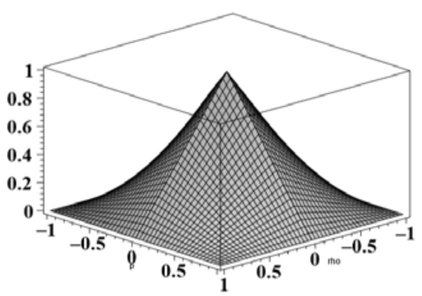

Fig. 13. Plot of real part of the basic function $V_{j,k}(\rho,\varphi) = w_j(\rho)\, v_k(\varphi)$.

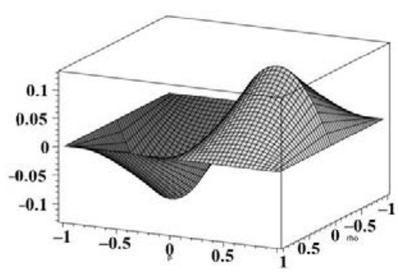

Fig. 14. Plot of imaginary part of the basic function $V_{j,k}(\rho,\varphi) = w_j(\rho) v_k(\varphi)$.

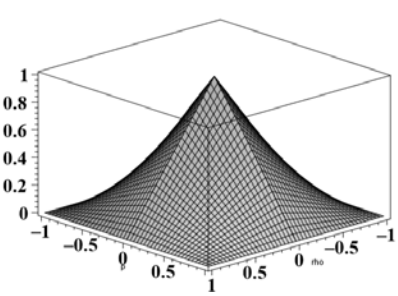

Fig. 15. Relief of the basic function $V_{j,k}(\rho,\varphi) = w_j(\rho) v_k(\varphi)$.

Further, we compare approximation $\tilde{u}_1(\rho,\varphi)$ with the following:

$$\begin{aligned}\tilde{u}_2(\rho,\varphi) &= u(r_j,\varphi_k)\, w_j(\rho)\, v_k(\varphi) + \\ &+ u(r_{j+1},\varphi_{k+1})\, w_{j+1}(\rho)\, v_{k+1}(\varphi) + \\ &+ u(r_{j+1},\varphi_k)\, w_{j+1}(\rho)\, v_k(\varphi) + \\ &+ u(r_j,\varphi_{k+1})\, w_j(\rho)\, v_{k+1}(\varphi) + \\ &+ u(r_{j+1},\varphi_{k-1})\, w_{j+1}(\rho)\, v_{k-1}(\varphi) + \\ &+ u(r_j,\varphi_{k-1})\, w_j(\rho)\, v_{k-1}(\varphi),\end{aligned} \tag{6}$$

where $w_j(\rho), w_{j+1}(\rho)$ are given in (5), and $v_s(\varphi)$, $s = k-1, k, k+1$ as follows:

$$v_k(\varphi) = \frac{(e^{I\varphi} - e^{I\varphi_{k-1}})(e^{I\varphi} - e^{I\varphi_{k+1}})}{(e^{I\varphi_k} - e^{I\varphi_{k-1}})(e^{I\varphi_k} - e^{I\varphi_{k+1}})},$$

$$v_{k+1}(\varphi) = \frac{(e^{I\varphi} - e^{I\varphi_{k-1}})(e^{I\varphi} - e^{I\varphi_k})}{(e^{I\varphi_{k+1}} - e^{I\varphi_{k-1}})(e^{I\varphi_{k+1}} - e^{I\varphi_k})}, \tag{7}$$

$$v_{k-1}(\varphi) = \frac{(e^{I\varphi} - e^{I\varphi_k})(e^{I\varphi} - e^{I\varphi_{k+1}})}{(e^{I\varphi_{k-1}} - e^{I\varphi_k})(e^{I\varphi_{k-1}} - e^{I\varphi_{k+1}})}.$$

For comparison, we also consider the approximation in the form:

$$\begin{aligned}\tilde{u}_3(\rho,\varphi) &= u(r_j,\varphi_k) w_j(\rho) v_k(\varphi) + \\ &+ u(r_{j+1},\varphi_{k+1}) w_{j+1}(\rho) v_{k+1}(\varphi) + \\ &+ u(r_{j+1},\varphi_k) w_{j+1}(\rho) v_k(\varphi) + \\ &+ u(r_j,\varphi_{k+1}) w_j(\rho) v_{k+1}(\varphi) + \\ &+ u(r_{j+1},\varphi_{k-1}) w_{j+1}(\rho) v_{k-1}(\varphi) + \\ &+ u(r_j,\varphi_{k-1}) w_j(\rho) v_{k-1}(\varphi) + \\ &+ u(r_{j-1},\varphi_{k-1}) w_{j-1}(\rho) v_{k-1}(\varphi) + \\ &+ u(r_{j-1},\varphi_k) w_{j-1}(\rho) v_k(\varphi) + \\ &+ u(r_{j-1},\varphi_{k+1}) w_{j-1}(\rho) v_{k+1}(\varphi),\end{aligned} \tag{8}$$

where $v_s(\varphi)$, $s = k-1, k, k+1$ are given in (7), and we take $\omega_j(x)$, $\omega_s^T(\rho)$, $\omega_s^E(\rho)$, instead of $w_s(\rho)$

Example 3. We denote

$$R^r = \max_K |\operatorname{Re}(\tilde{u}(\rho,\varphi)) - \operatorname{Re}(u(\rho,\varphi))|,$$

$$R^i = \max_K |\operatorname{Im}(\tilde{u}(\rho,\varphi)) - \operatorname{Im}(u(\rho,\varphi))|.$$

Let us find the approximation of function $u(\rho,\varphi) = \sin(\rho e^{I\varphi}) = A(\rho,\varphi) + I\, B(\rho,\varphi)$, where

$A(\rho,\varphi) = \sin(\rho\cos(\varphi))\cosh(\rho\sin(\varphi))$,

$B(\rho,\varphi) = \cos(\rho\cos(\varphi))\sinh(\rho\sin(\varphi))$.

If $w_s(\rho)=\omega_j(\rho)$, $n=10, m=10$ we obtain: $R^r \le 0.086$, $R^i \le 0.067$ when we use approximation (4), $R^r \le 0.031$, $R^i \le 0.030$ when we use approximation (6), and $R^r \le 0.015$, $R^i \le 0.016$, when we use approximation (8).

A plot of the approximation of real part $u(\rho,\varphi)=\sin(\rho e^{I\varphi})$, when we use approximation (4), is given in Fig. 16. Errors of approximations of the real and the imaginary parts of functions with spline (6) are given in Table 3I, when $n=10$, $m=10$.. Errors of approximation of the real and the imaginary parts of the functions with splines (4) are given in Table 4, when $n=100$, $m=100$. The calculations are done in Maple, Digits=15. Suppose *n*=10, *m*=10.

Example 4. Let us take $n=10, m=10$. If we take exponential splines along the radial variable: $w_s(\rho)=\omega_s^E(\rho)$, we obtain the errows of approximation presented in Table 5. If we take polynomial splines along radial variable: $w_s(\rho)=\omega_j(\rho)$, we obtain the errows of approximation presented in Table 6. If we take trigonometrical splines along radial variable: $w_s(\rho)=\omega_s^T(\rho)$, we obtain the errows of approximation presented in Table 7. A plot of the errors of approximation of real part $u(\rho,\varphi)=\sin(\rho e^{I\varphi})$, when we use approximation (4), is given in Fig. 17. A plot of the errors of approximation of real part $u(\rho,\varphi)=\sin(\rho e^{I\varphi})$, when we use approximation (8), is given in Fig. 18.

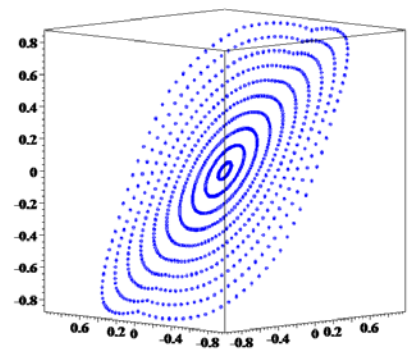

Fig. 16. Plot of the real part of function $u(\rho,\varphi)=\sin(\rho e^{I\varphi})$ with spline (4), *n=10, m=10.*

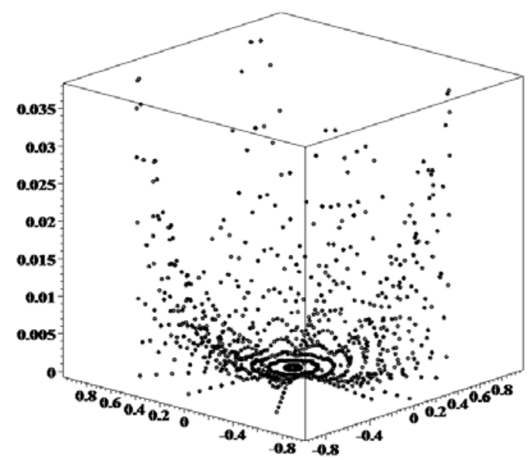

Fig. 17. Plot of the errors of approximation of the real part of function $u(\rho,\varphi)=\sin(\rho e^{I\varphi})$ with spline (4), *n*=10, *m*=10.

TABLE 3 ERRORS OF APPROXIMATION OF FUNCTIONS $u(\rho,\varphi)$ WITH SPLINES (8), WHEN $w_s(\rho)=\omega_j(\rho)$, $n=10, m=10$

$u(\rho,\varphi)$	R^r	R^i
$\cos(\rho e^{I\varphi})$	$0.11\cdot10^{-1}$	$0.11\cdot10^{-1}$
$\sin(2\rho e^{I\varphi})$	0.21	0.21
$\rho^3 e^{3I\varphi}$	$0.75\cdot10^{-1}$	$0.77\cdot10^{-1}$

TABLE 4 ERRORS OF APPROXIMATION OF FUNCTIONS $u(\rho,\varphi)$ WITH SPLINES (4), WHEN $n=100, m=100$

$u(\rho,\varphi)$	R^r	R^i
$\cos(\rho e^{I\varphi})$	$0.77\cdot10^{-3}$	$0.65\cdot10^{-3}$
$\sin(2\rho e^{I\varphi})$	$0.66\cdot10^{-2}$	$0.73\cdot10^{-2}$
$\rho^3 e^{3I\varphi}$	$0.30\cdot10^{-2}$	$0.30\cdot10^{-2}$

TABLE 5. ERRORS OF APPROXIMATION OF FUNCTIONS $u(\rho,\varphi)$ WITH SPLINES (8), WHEN $w_s(\rho)=\omega_s^E(\rho)$, $n=10, m=10$

$u(\rho,\varphi)$	R^r	R^i
$\exp(3\rho)\exp(2i\varphi)$	$0.60\cdot10^{-2}$	$0.60\cdot10^{-2}$
$\sin(3\rho)\exp(2i\varphi)$	$0.22\cdot10^{-2}$	$0.22\cdot10^{-2}$
$\sin(2\rho)\exp(2i\varphi)$	$0.82\cdot10^{-3}$	$0.81\cdot10^{-3}$

TABLE 6. ERRORS OF APPROXIMATION OF FUNCTIONS $u(\rho,\varphi)$ WITH SPLINES (8), WHEN $w_s(\rho)=\omega_s(\rho)$, $n=10, m=10$

$u(\rho,\varphi)$	R^r	R^i
$\exp(3\rho)\exp(2i\varphi)$	$0.26\cdot10^{-1}$	$0.26\cdot10^{-1}$
$\sin(3\rho)\exp(2i\varphi)$	$0.17\cdot10^{-2}$	$0.17\cdot10^{-2}$
$\sin(2\rho)\exp(2i\varphi)$	$0.50\cdot10^{-3}$	$0.50\cdot10^{-3}$

TABLE 7. ERRORS OF APPROXIMATION OF FUNCTIONS $u(\rho,\varphi)$ WITH SPLINES (8), WHEN $w_s(\rho)=\omega_s^T(\rho)$, $n=10$, $m=10$

$u(\rho,\varphi)$	R^r	R^i
$\exp(3\rho)\exp(2i\varphi)$	$0.29\cdot10^{-1}$	$0.29\cdot10^{-1}$
$\sin(3\rho)\exp(2i\varphi)$	$0.15\cdot10^{-2}$	$0.15\cdot10^{-2}$
$\sin(2\rho)\exp(2i\varphi)$	$0.37\cdot10^{-3}$	$0.37\cdot10^{-3}$

The results presented in Tables 5-7 show that trigonometrical splines can provide better approximation for trigonometrical functions, and exponential splines can provide better approximation for exponential functions.

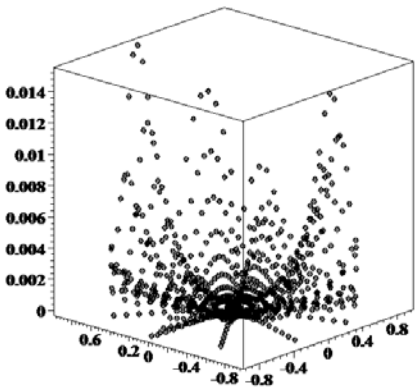

Fig. 18. Plot of the errors of approximation of the real part of function $u(\rho,\varphi)=\sin(\rho e^{I\varphi})$ with spline (7), n=10, m=10.

Suppose n=100, m=100. A plot of the error approximations of real part $u(\rho,\varphi)=\sin(\rho e^{I\varphi})$ when we use approximation (4), is given in Fig. 19.

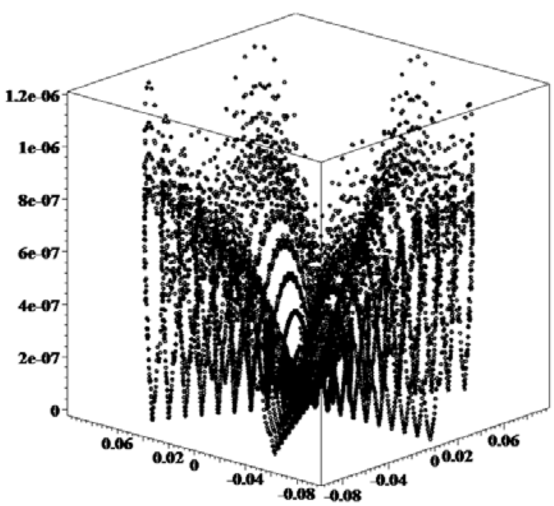

Fig. 19: Plot of the errors of approximation of the real part of function $u(\rho,\varphi)=\sin(\rho e^{I\varphi})$ with splines (4), n=100, m=100.

Suppose n=10, m=10. A plot of the real part $u(\rho,\varphi)=\sin(2\rho)\exp(\rho e^{2I\varphi})$ when we use approximation (8), is given in Fig.20. The plots of the error approximations of the real and the imaginary parts $u(\rho,\varphi)=\sin(2\rho)\exp(\rho e^{2I\varphi})$ when $w_s(\rho)=\omega_s^T(\rho)$, and we use approximation (8), are given in Fig.21,22.

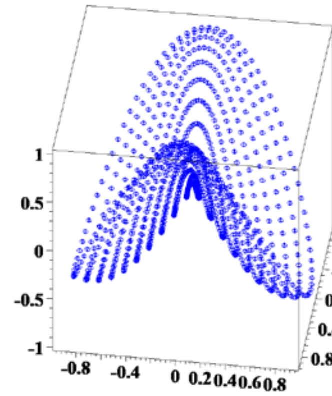

Fig.20. The real part $u(\rho,\varphi)=\sin(2\rho)\exp(\rho e^{2I\varphi})$ when $w_s(\rho)=\omega_s^T(\rho)$, and we use approximation (8)

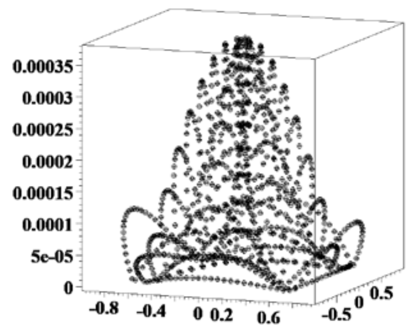

Fig.21. The plot of the error approximations of the real part $u(\rho,\varphi)=\sin(2\rho)\exp(\rho e^{2I\varphi})$ when $w_s(\rho)=\omega_s^T(\rho)$, and we use approximation (8)

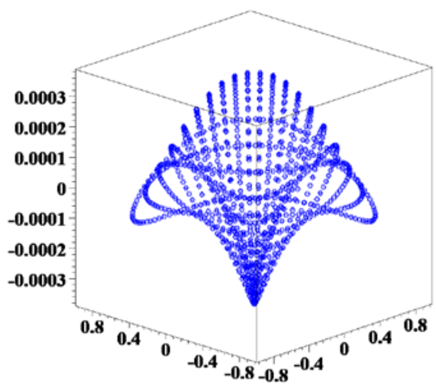

Fig.22. The plot of the error approximations of the image part $u(\rho,\varphi)=\sin(2\rho)\exp(\rho e^{2I\varphi})$ when $w_s(\rho)=\omega_s^T(\rho)$, and we use approximation (8)

IV. IMAGE RESIZING

Paper [28] noted that "the full color image contains three components (Red, Green and Blue) in each pixel, but a Bayer image, which is the output of a Bayer CFA, contains only one component in each pixel. However, from a Bayer image a full color image is generated by demosaicing, that is, an interpolation that estimates the values of the missing components”. In solving this problem, local splines considered in this paper can be very useful. One more important task is to compress the image for compact storage or transfer it to a distance and then restore it. We used polynomial and trigonometrical splines for compressing and restoring images. The considered splines can be used to solve this problem. Another task is to resize the image in accordance with the properties of various modern displays. In short, the algorithm for increasing the size of the image is as such: we associate every pixel in a row of the original image to a pixel of the enlarge imaged in a row for every color (Red, Green, Blue) as it is shown in Fig.23. Then information about the color in the row will look as it does in Fig.24.

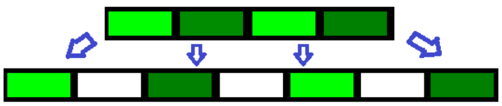

Fig.23. The process of increasing the size

Fig.24. The information about the colors in the row

Fig.25. New information about the colors in the row

Here the intermediate pixel in white has no information about the color. Using the spline approximation we can calculate the values in intermediate pixels (see Fig.25). We construct the approximation to the left side of the row with the right splines. We construct the approximation to the right side of the row with the left splines. Then we repeat the procedure for the columns: for the upper part we construct the approximation with the right splines whereas to the lower part we construct the approximation with the left splines. Thus, we calculate all the color values in the all pixels of enlarged image (calculations are performed for each color component: red, green, blue). The process can be parallelized.

Fig.26 shows the original image. Fig.27 shows the enlarged image constructed using polynomial splines. The original image is doubled. The original image was taken from the site https://pixabay.com/. Applying the proposed splines, the image can be enlarged not only twice, but also more times. Note that with an increase in a greater number of times to improve the image quality, it is advisable to use splines of a higher approximation order. The following papers will be devoted to this issue.

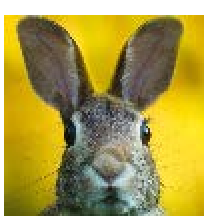

Fig.26. The original image

Fig.27. The enlarged image

V. Conclusion

In this paper, the features of approximation by splines of one variable and complex-valued splines are considered. An approximation in the disc is constructed with the help of the tensor product of polynomial real splines along the radial component and complex exponential splines along the circle. The results of the numerical experiments (Tabl. 1,2) show the numerical stability of the proposed approximation approach. In future papers, the values of the constants in the error estimates will be refined.

The proposed local representation of information about a curve or surface can be used to compress information. Compressed information can be stored or transmitted in a compact form. In addition to arrays of nodes and values of functions in them the subsequent reconstruction is also necessary to have formulas of basic splines.

References

[1] J.H. Ahlberg, E. N. Nilson, J. L. Walsh, *Theory of Splines and Their Applications*, Mathematics in Science and Engineering, Chapt. IV. Academic Press, New York, 1967.

[2] Carl de Boor, *A practical guide to splines*, Applied Mathematical Science, Springer-Verlag,New York, Heidelberg. Berlin, , vol.27, 1978.

[3] J.L.Walsh, *Interpolation and approximation*, 3rd ed., Amer. Math. Soc. Colloquium Publications., vol. 20, Amer. Math. Soc, Providence, R.L, 1960.

[4] J.H. Ahlberg, E. N. Nilson, J. L. Walsh, “Complex cubic splines,” Trans. Amer. Math. Soc., vol. 129, 1967, pp. 391-413.

[5] J.H. Ahlberg, Splines in the Complex Plane, “Approximations with Special Emphasis on Spline Functions,” Academic Press, New York, 1969, pp.1-27.

[6] J.L. Walsh, “Interpolation and approximation by rational functions in the complex domain,” American Math. Society, Colloquium Publications, Providence, RI, vol. 20, 382 p., 1956.

[7] L. Reichel, “On polynomial approximation in the complex plane with application to conformal mapping,” Mathematics of Computation, vol. 44, 1985, pp. 425-433.

[8] B.Forster, Thierry Blu, Michael Unser, “Complex B-splines,” Applied and Computational Harmonic Analysis, vol. 20, 2006, pp. 261-282.

[9] B. Forster, R. Garunkstis, P. Massopust and J. Steuding, “Complex B-splines and Hurwitz zeta functions,” LMS Journal of Computation and Mathematics, vol. 16, 2013, pp. 61-77.

[10] Chen Han- Lin, “Complex spline functions,” Sei. Sonica, No. 2, vol. 24, 1981, pp. 160-169.

[11] Chen Han - Lin, Tron Hvaring, "A New Method for the Approximation of Conformai Mapping on the Unit Circle," Mathematics of Computation, No. 6, 1982, pp. 151-164.

[12] M.A. Lawrentjew, B. W. Schabat, *Methoden der komplexen Funktionentheorie*, VEB Deutscher Verlag der Wissenschaften, Berlin, 1967.

[13] S. Sargheini, A. Paganini, R. Hiptmair, C. Hafner, "Shape sensitivity analysis of metallic nano particles", International Journal of Numerical Modelling: Electronic Networks, Devices and Fields, vol. 30, Issue 5, 2017.

[14] S. Chen, X. Hong, E.F. Khalaf, A. Morfeq, N.D. Alotaibi, C.J. Harris, "Single-Carrier Frequency-Domain Equalization with Hybrid Decision Feedback Equalizer for Hammerstein Channels," Containing Nonlinear Transmit Amplifier IEEE Transactions on Wireless Communications, vol. 16, Issue 5, pp.3341-3354, May 2017.

[15] S. Chen, X. Hong, J. Gao, C.J. Harris, "Complex-valued B-spline neural networks for modeling and inverting hammerstein systems," IEEE Transactions on Neural Networks and Learning Systems, vol. 25, Issue 9, pp.1673-1685, September 2014.

[16] X. Hong, S. Chen, C.J. Harris, "B-spline neural network based single-carrier frequency domain equalisation for Hammerstein channels," Proceedings of the International Joint Conference on Neural Networks, pp. 1834-1841, 2014.

[17] C. Apprich, A. Dieterich, K. Höllig, E. Nava-Yazdani, "Cubic spline approximation of a circle with maximal smoothness and accuracy," Computer Aided Geometric Design, vol. 56, pp 1-3, 2017.

[18] M. I. Ganzburg, "Exact errors of best approximation for complex-valued periodic functions," Journal of Approximation Theory, vol. 229, 2018, pp. 1- 12.

[19] Leslie Ann Goldberg, Heng Guo, "The Complexity of Approximating complex-valued Ising and Tutte partition functions," Journal Computational Complexity archive, vol. 26, Issue 4, 2017, pp 765-833.

[20] T. Magesacher, P. Singerl, M. Mataln, "Optimal Segmentation for Piecewise RF Power Amplifier Models," IEEE Microwave and Wireless Components Letters, vol. 26, Issue 11, pp. 909-911, 2016.

[21] X.Hong, S. Chen, C.J. Harris, "Complex-Valued B-Spline Neural Networks for Modeling and Inverse of Wiener Systems," Complex-Valued Neural Networks: Advances and Applications, 2013, pp. 209-234.

[22] D.Chazot, B. Nennig, E. Perrey-Debain, "Performances of the Partition of Unity Finite Element Method for the analysis of two-dimensional interior sound fields with absorbing materials," Journal of Sound and Vibration, 332 (8) , 2013, pp.1918-1929.

[23] H.P.Moon, R.T.Farouki, "C1 and C2 interpolation of orientation data along spatial Pythagorean-hodograph curves using rational adapted spline frames", Computer Aided Geometric Design, 66, 2018, pp.1-15.

[24] X. Hong, S. Chen, " Modeling of complex-valued wiener systems using B-spline neural network," IEEE Transactions on Neural Networks,22(5), pp.818-825, 2011.

[25] I.G. Burova, "Approximation by complex splines," Vestnik Leningradskogo Universiteta, Seriya Matematika, Mekhanika Astronomiya, vol. 2, 1986, pp. 3-9.

[26] Burova, I.G, "On left integro-differential splines and Cauchy problem," International Journal of Mathematical Models and Methods in Applied Sciences, vol. 9, 2015, pp. 683-690

[27] I.G.Burova, S.V.Poluyanov, "On approximations by polynomial and trigonometrical integro-differential splines", International Journal of Mathematical Models and Methods in Applied Sciences, vol.10, 2016, pp.190-199.

[28] Z.Li, P.Z.Revesz, "Bilinear and smooth hue transition interpolation-based bayer filter designs for digital cameras," International Journal of Circuits, Systems and Signal Processing, 2015, vol.9, pp. 211-221.